

# CO and [CII] along NGC 7479's bar\*

**Dario Fadda**

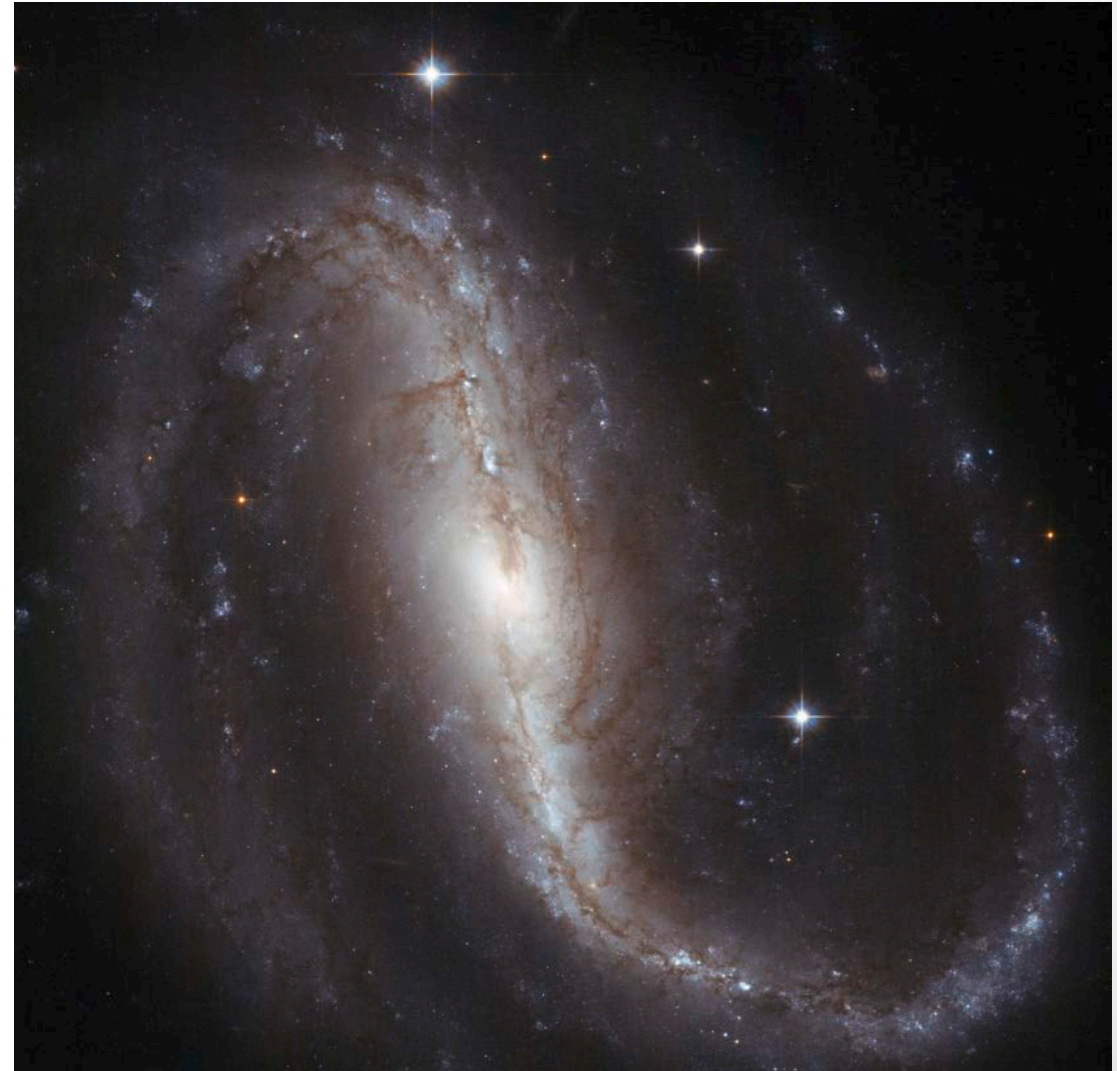
(SOFIA Science Center)

**Seppo Laine**

**Phil Appleton**

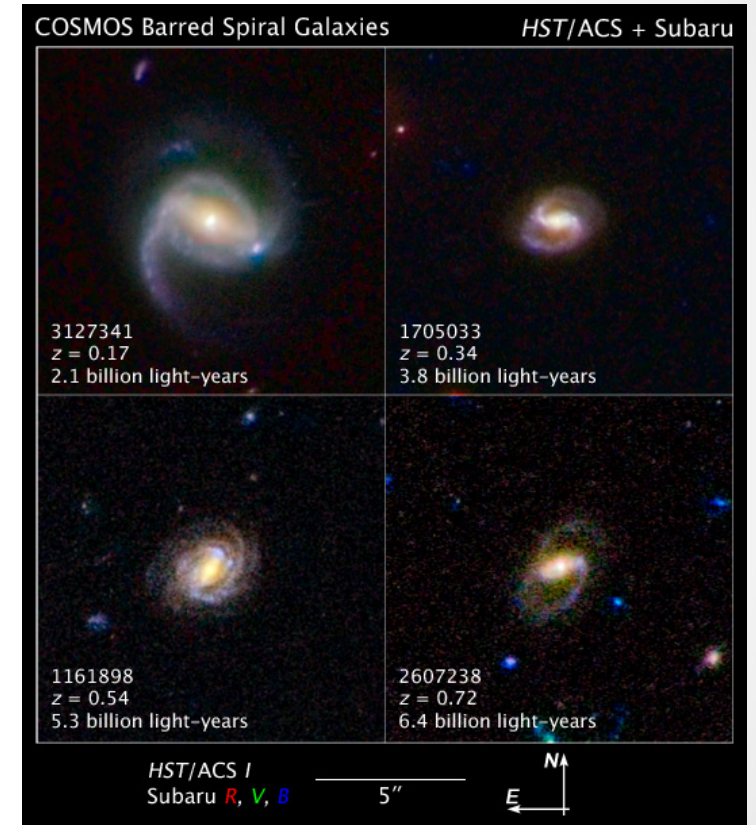
(IPAC, Caltech)

27 January 2021



# Barred galaxies

- 70% of spiral galaxies in local Universe are barred (Eskridge+ 2000)
- This percentage declines at higher redshifts (Sheth+ 2008)
- Many spirals have small companions which can merge
- Minor mergings can favor bar creation (Mihos & Hernquist 1994)
- Minor mergings lead to central active nuclei (Taniguchi 1999)
- Observations show that bars funnel gas to the nucleus
- Along bars there is a dearth of HI, depleted by SF and transition to H<sub>2</sub>
- H $\alpha$  is limited to regions of active SF and is attenuated by dust
- Best way to study bars is to trace the molecular gas with CO and C<sup>+</sup>



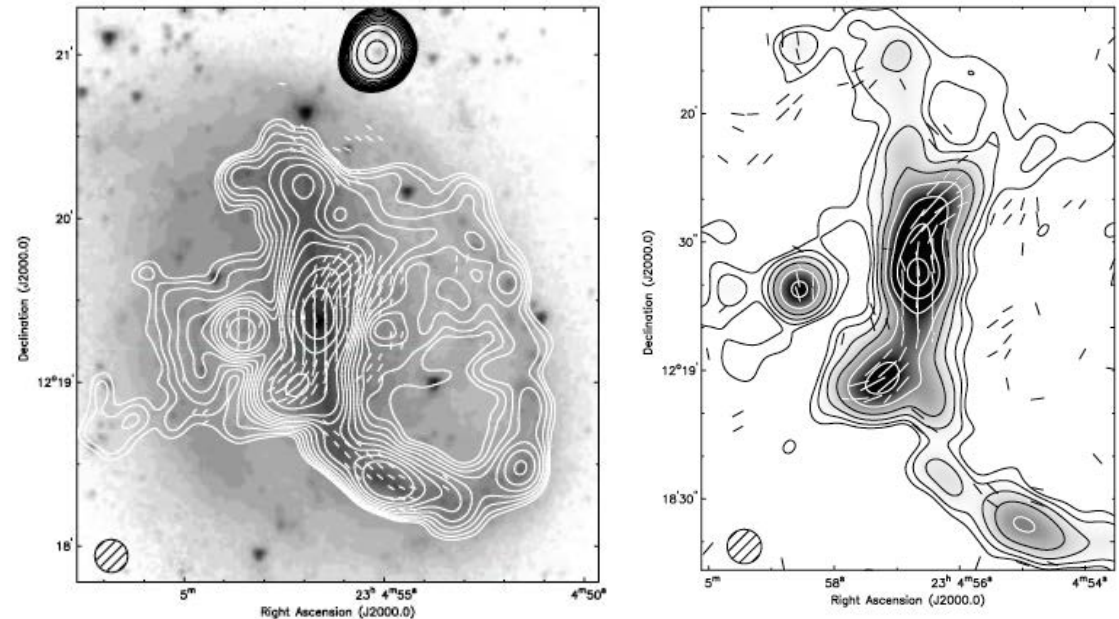
COSMOS barred galaxies from Sheth+ 2008

# NGC 7479

- Distance:  $cz = 2371$  km/s
- Barred asymmetric (strong western arm), presence of horizontal dust lanes (minor merging, Laine & Heller 1999)
- Sy 1.9 (Ho+ 1997)
- Absence of HI emission along the bar (Laine & Gottesman, 1998)
- Radio counter-arms linked to jets. Polarization: B aligned with jets (Laine & Beck 2008). The counter-arms were not detected in XMM observations.



HI map vs  $r'$  map (Laine & Gottesman 1998)

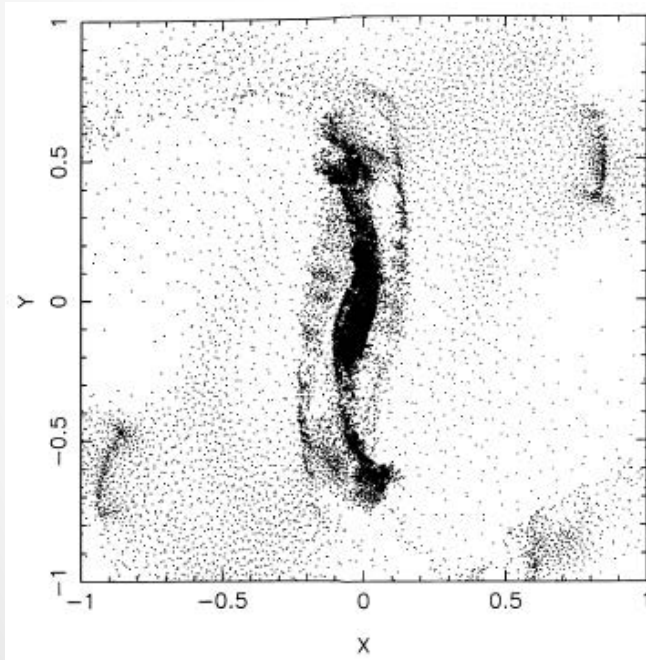


Radio continuum maps & polarization (Laine & Beck 2008)

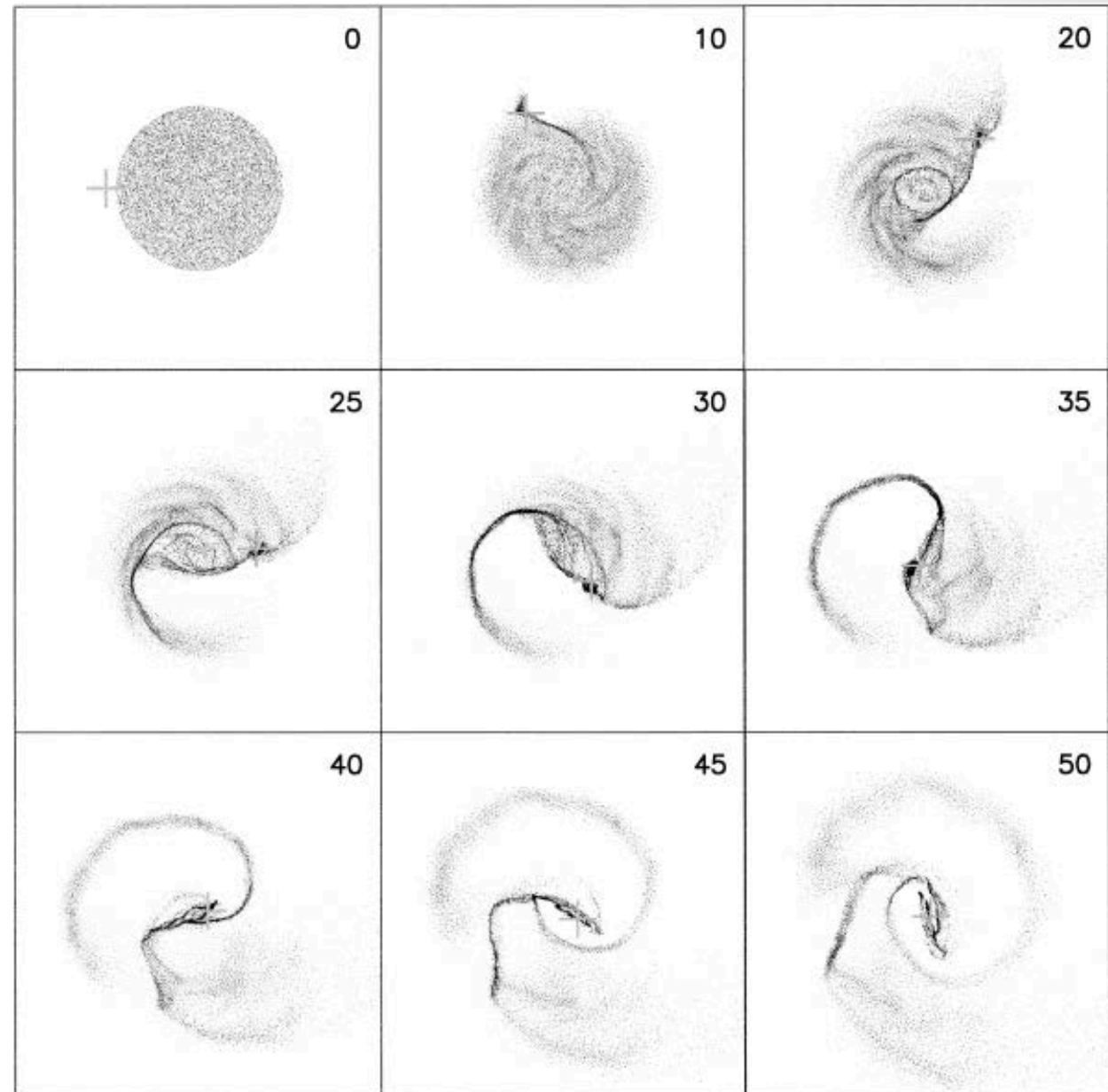


# Models

- Model of bar pattern speed.  
High speed rotator  $\Omega_p \sim 27$  km/s  
(Laine+ 1998)
- Minor-merger model (Laine & Heller 1999)

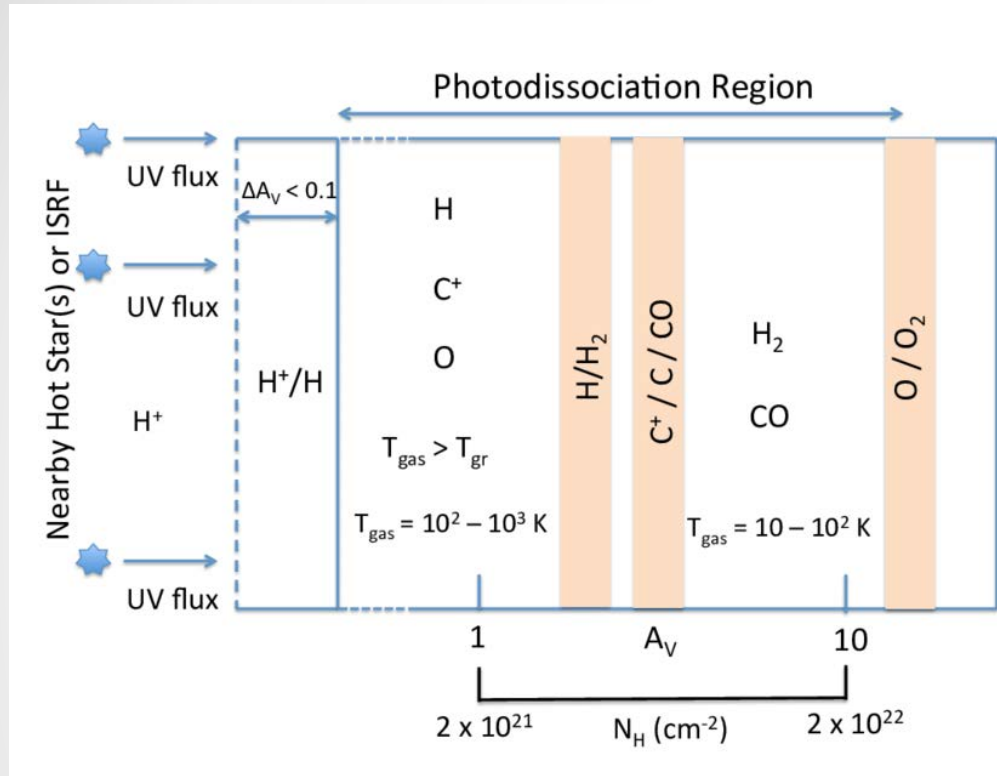


Laine+ 1998



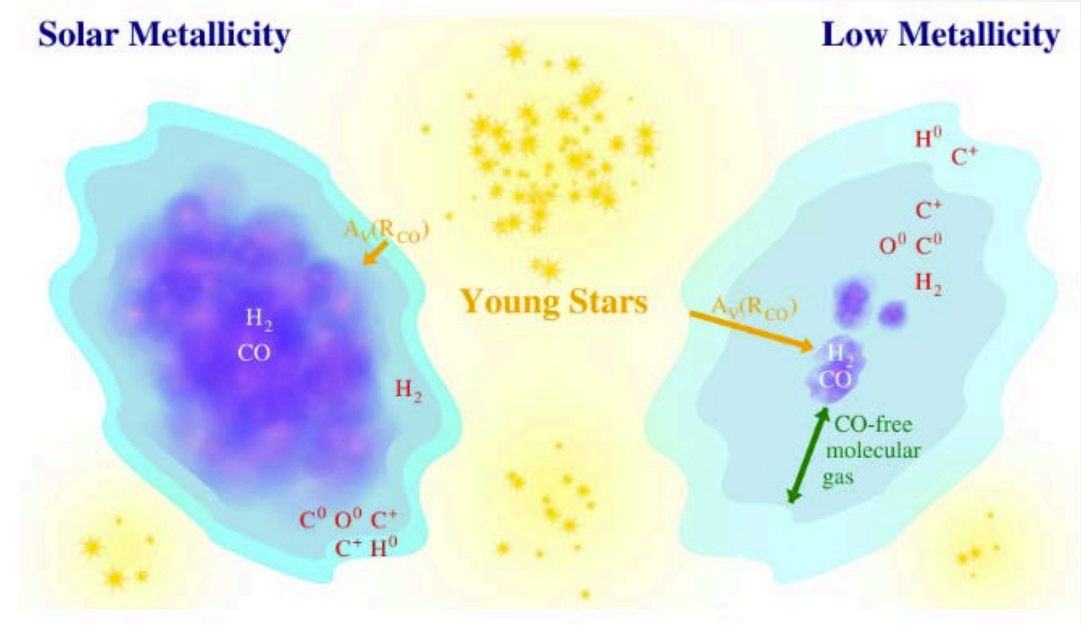
Laine & Heller 1999

# Origin of CO and [CII] emission



PDR (Hollenbach & Tielens 1999)

Since the lowest transitions of  $\text{H}_2$  have excitation energies of  $E/k \sim 500\text{K}$  and  $1000\text{K}$ , cold  $\text{H}_2$  can be only detected indirectly from C, O, and CO emission. The ground rotational transition of CO (2.6 mm) is easily excitable since requires a low excitation energy: 5.5 K. C has low ionization potential (11.3 eV) and  $\text{C}^+$  is relatively easy to excite (92 K). It emits a very intense line in the IR ( $158\mu\text{m}$ ).



CO dark regions (Madden+ 2020)

In low metallicity regions, while  $\text{H}_2$  can self-shield, CO needs grains of dust to shield it from photodissociation. So, some of the  $\text{H}_2$  gas can be CO free and  $\text{H}_2$  can be better traced by  $\text{C}^+$ .

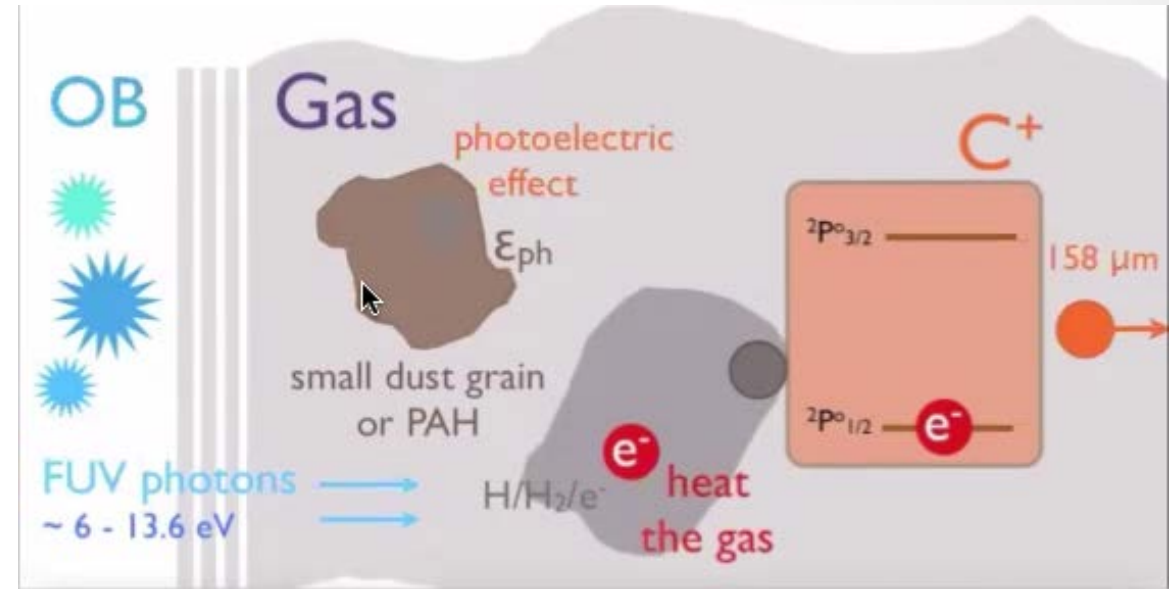
# Photo-electric effect

- 60-80% of the C<sup>+</sup> emission comes from neutral H and H<sub>2</sub> (Croxall+ 2017).

C<sup>+</sup> emission is due to excitation with collision of H and H<sub>2</sub>. These atoms and molecules are heated by e<sup>-</sup> released from PAHs and small grains hit by UV radiation. The emission from C<sup>+</sup> atoms cools the gas.

Because of this mechanism, there is usually a good relationship between PAH emission and C<sup>+</sup> emission.

- A small part of C<sup>+</sup> emission comes from HII regions where free electrons excite the C<sup>+</sup> with collisions.



(Herrera-Camus)

<https://www.youtube.com/watch?v=SoZjymOsvsE>

Bakes & Tielens (1994), d'Hedencourt & Leger (1987)



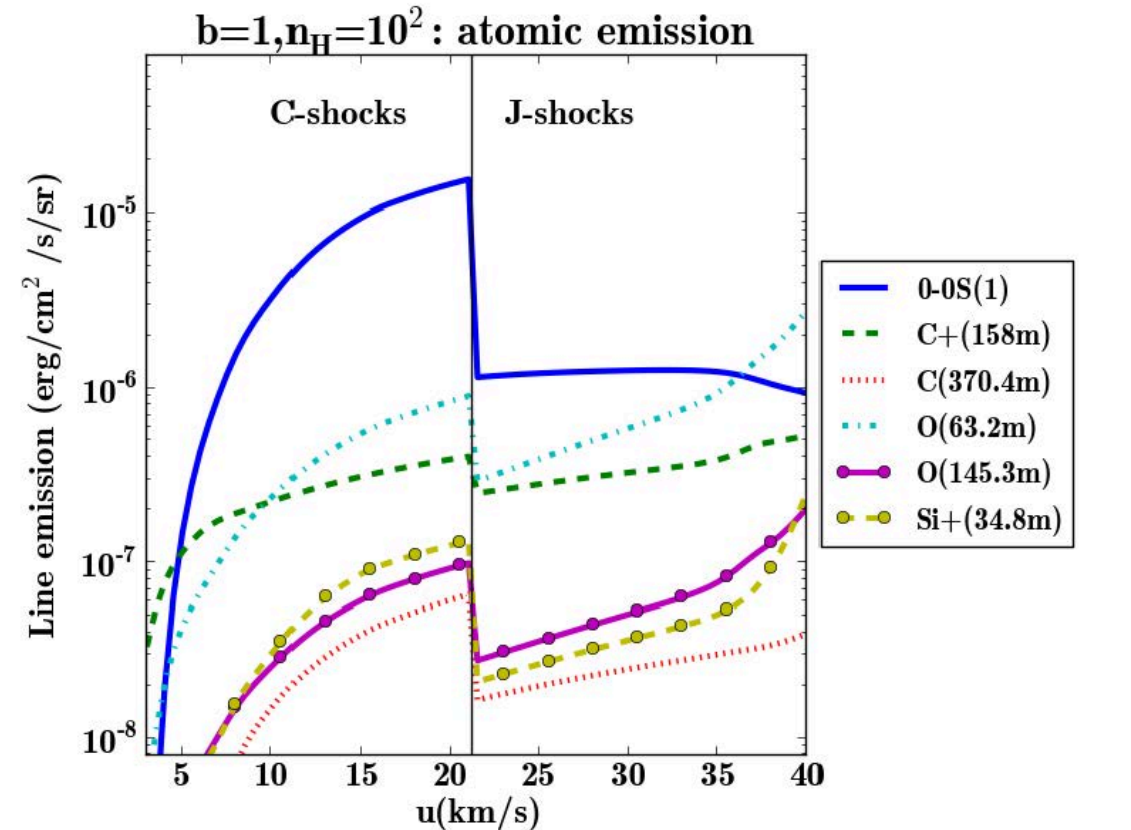
# Excitation by shocks

Another mechanism to excite  $C^+$  is through shocks in the molecular clouds.

Two types of shocks can be found in the ISM:

- J shocks, when the kinetic energy of a sharp velocity jump dissipates viscously
- C shocks, continuous degradation of kinetic energy into heat and photons via ion-neutral friction and cooling.

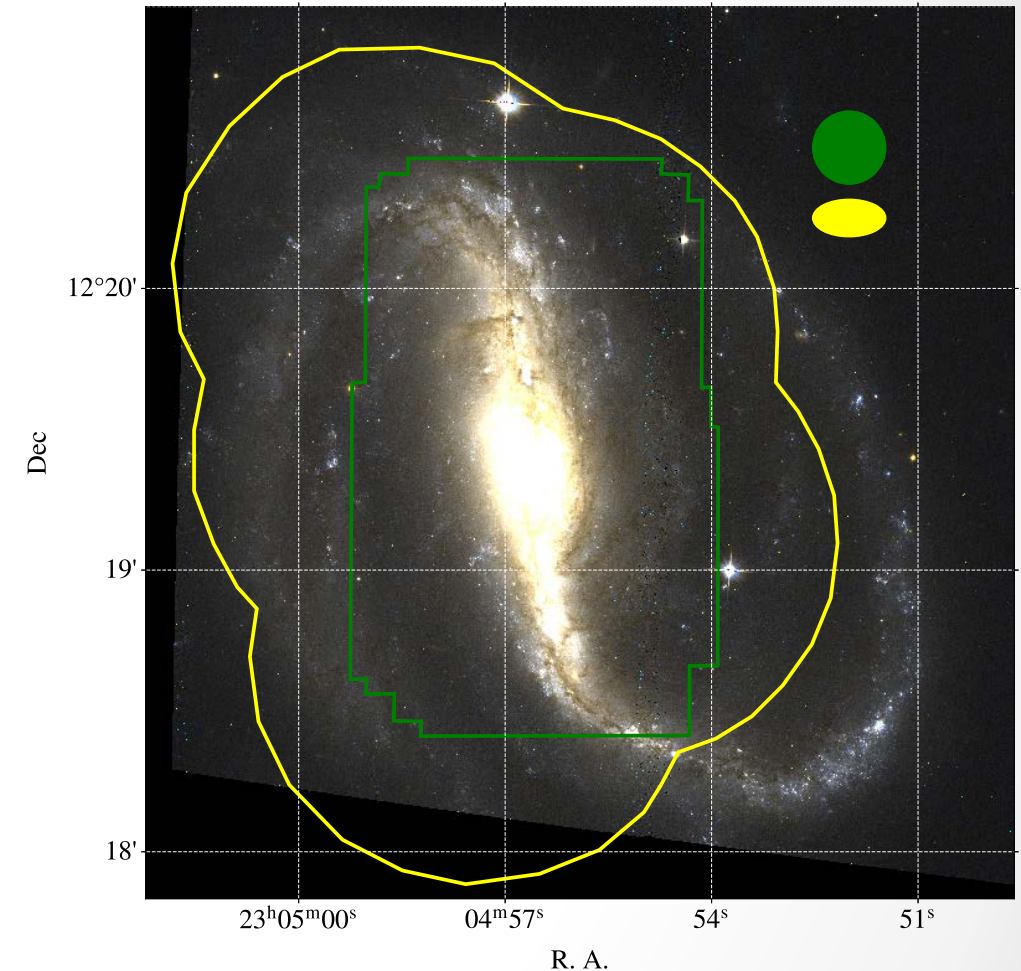
Simulations (Lesaffre+ 2013) predict intense  $C^+$  emission for low-velocity shocks, while [OI] emission becomes predominant in high velocity J shocks.



Lesaffre+ 2013

# Data

- [CII] – FIFI-LS/SOFIA (Cycle 7, May 2019)  
Exp: 2.5h. Res.: 257 km/s and 15.6".
- CO<sub>(J=1-->0)</sub> – ALMA Band 3, 7m array (2016)  
Exp: 1.43h. Res: 1.27 km/s and 15.6" x 8".
- Chandra obs. of SN1990U (10 ks) and SN2009JF (25 ks)
- Spitzer: IRAC and MIPS 24 $\mu$ m
- Herschel: PACS and SPIRE
- GALEX: NUV and FUV
- SDSS: 5 bands + spectrum
- 2MASS: 3 NIR bands
- H $\alpha$ : 1.5m Palomar – Fabry Perot spec by Vogel & Regan (1994)  
Exp: 40 x 500s. Res: 12.1 km/s and 3.6"



NGC 7479 with [CII] (green, FIFI-LS/SOFIA) and CO (yellow, ALMA) coverage.



# Nuclear activity

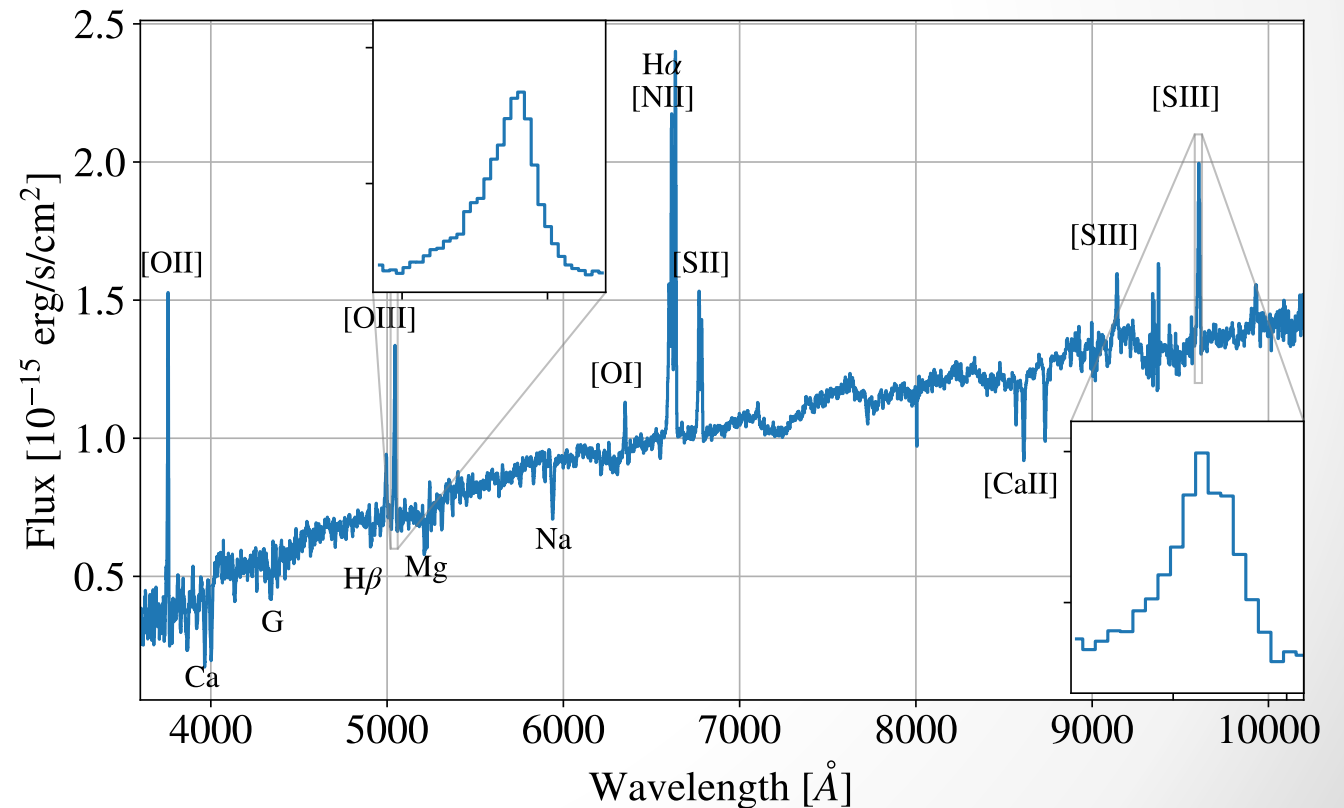
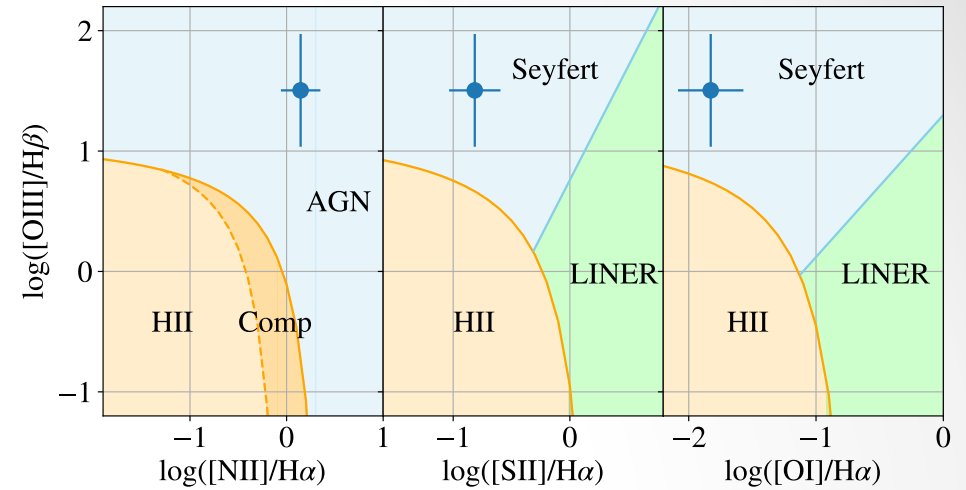
We analyzed a recent SDSS spectrum of the nucleus (2012).

The nucleus hosts a Seyfert AGN according to the Kewley+ (2006) diagrams.

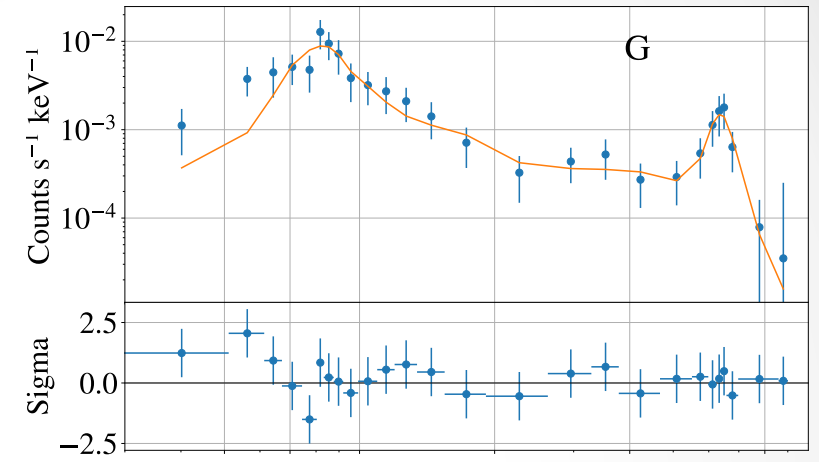
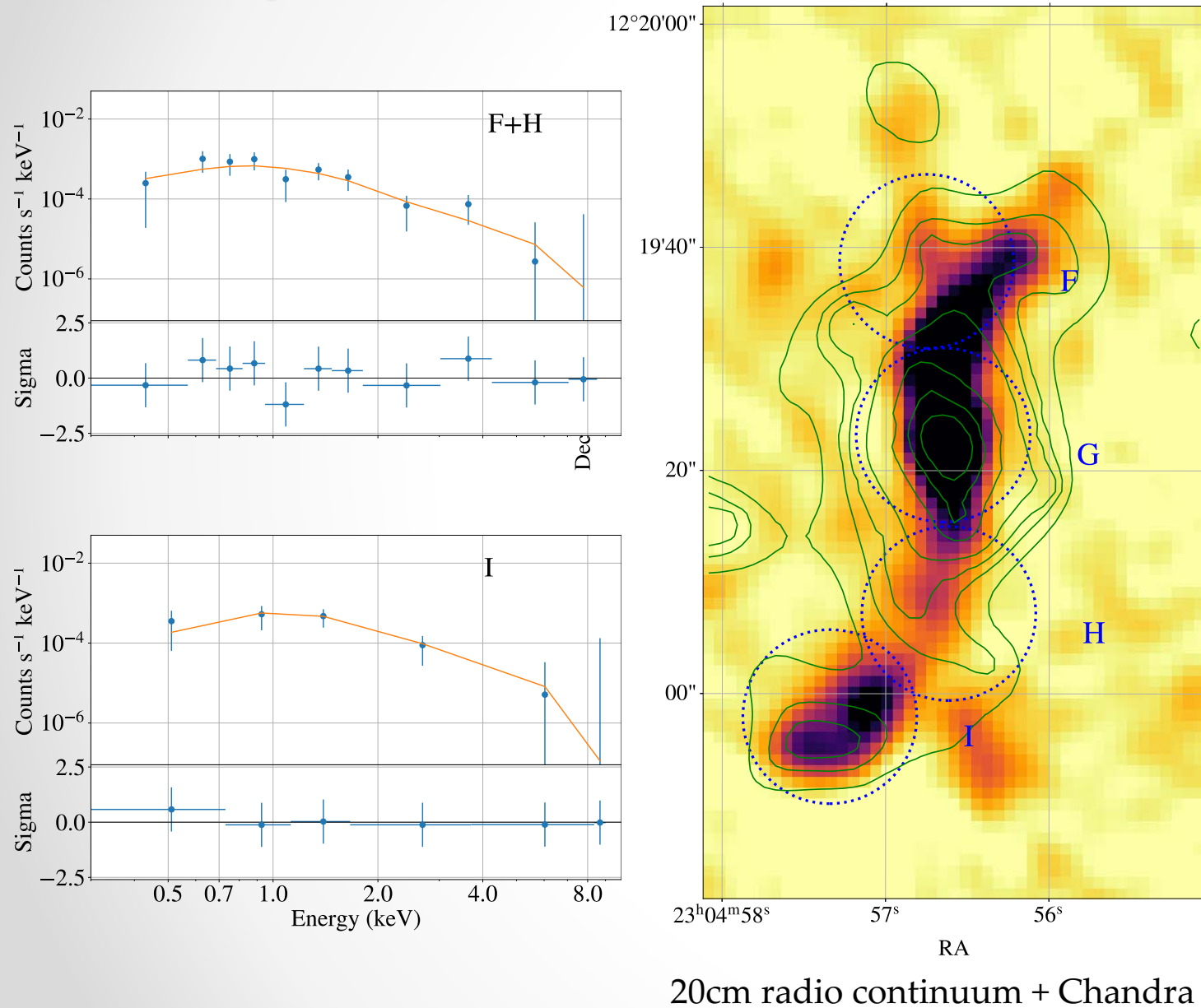
Line ratio  $H\beta/[OIII] = 0.22 \pm 0.10$ , so it is a Sy 1.8 according to Winkler (1992).

High extinction ( $A_V = 8.4$ ) from Balmer ratio, typical of Sy 1.8-2.

Narrow lines  $[OIII]5008$  and  $[SIII]9068$  have blue wings, usually associate to gas outflows.



# X-ray detection with Chandra



Chandra observations (green) confirm the presence of counter-arms detected in the radio.

Nucleus typical AGN: prominent Fe  $K\alpha$  line at 6.4 keV and high HR=0.8.

Heavily obscured: broad profile of Fe line and high HI absorption ( $N_H=0.8 \times 10^{22} \text{ cm}^{-2}$ ).

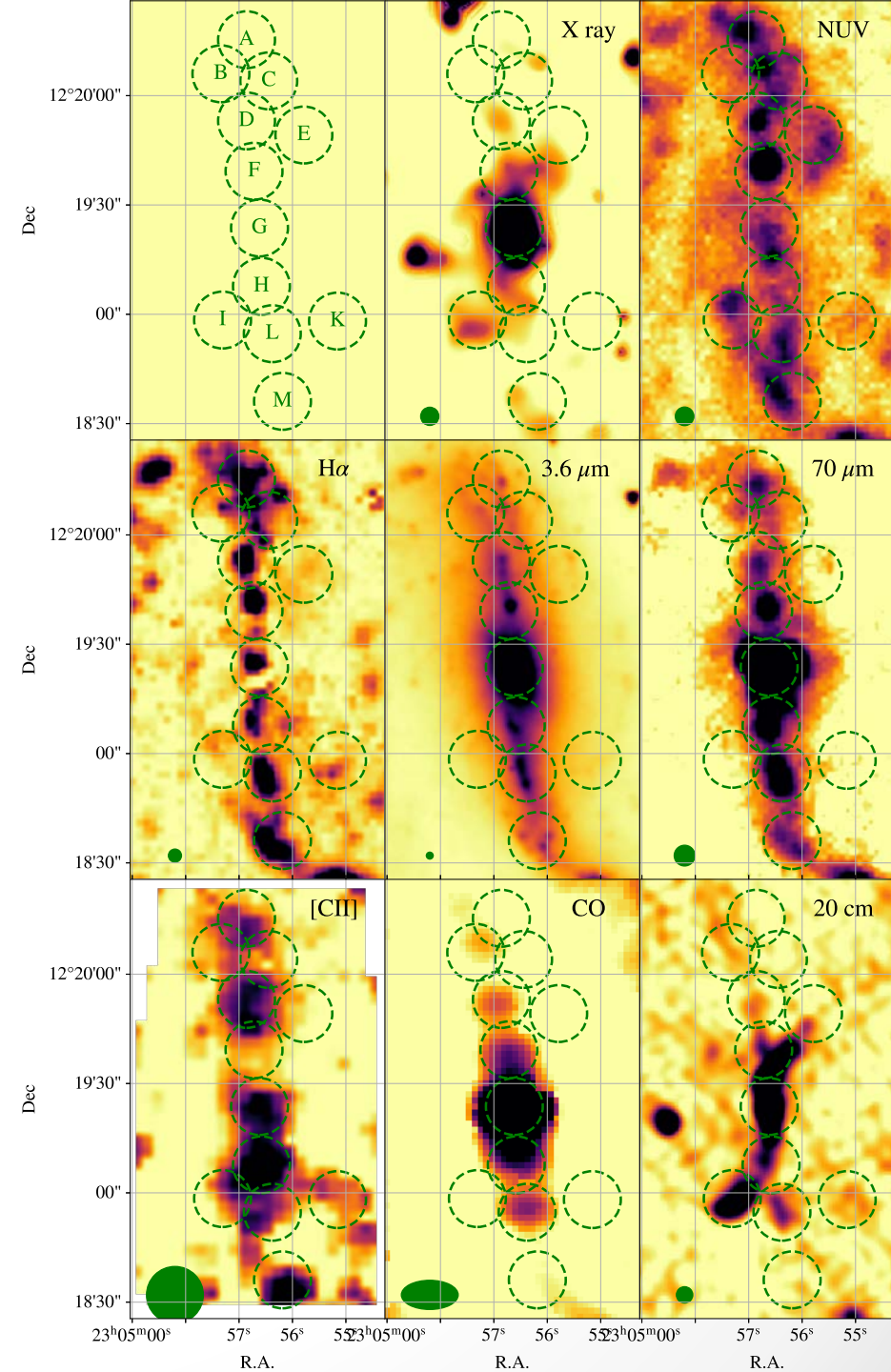
Emission in "F" and "G" can be explained with star formation. Emission in "I" too high to origin from star-formation only.

# A panchromatic view

To study this galaxy, we defined 12 circular apertures with diameter corresponding to the FWHM of FIFI-LS (15.6").

The apertures are centered in location of interest such as knots of star formation, radio hot spots, etcetera.

The fluxes are extracted after degrading the spatial resolution of other images to that of FIFI-LS.





# SED & spectra

For each aperture we fit MagPhys models (da Cunha+ 2008) to all the fluxes and fit Voigt profiles to the [CII] and CO spectra.

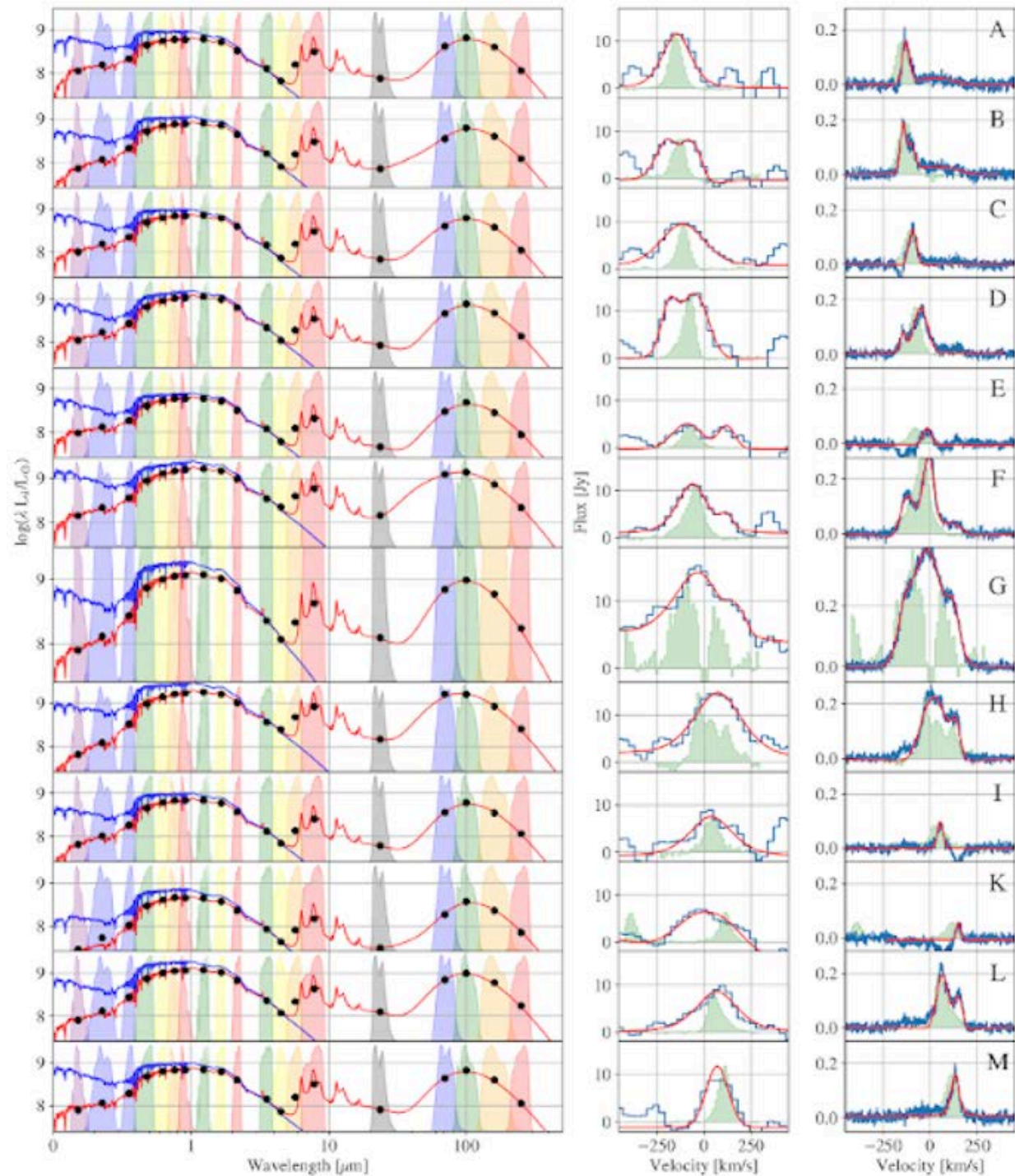
In the figure, the red line is the observed SED, while the blue line is the unattenuated SED computed by MagPhys, i.e. the radiation expected if dust was not present in the system.

Spectra:

[CII]: middle column

CO: left column

The green shade corresponds to the H $\alpha$  line rescaled to the intensity of [CII] or CO.

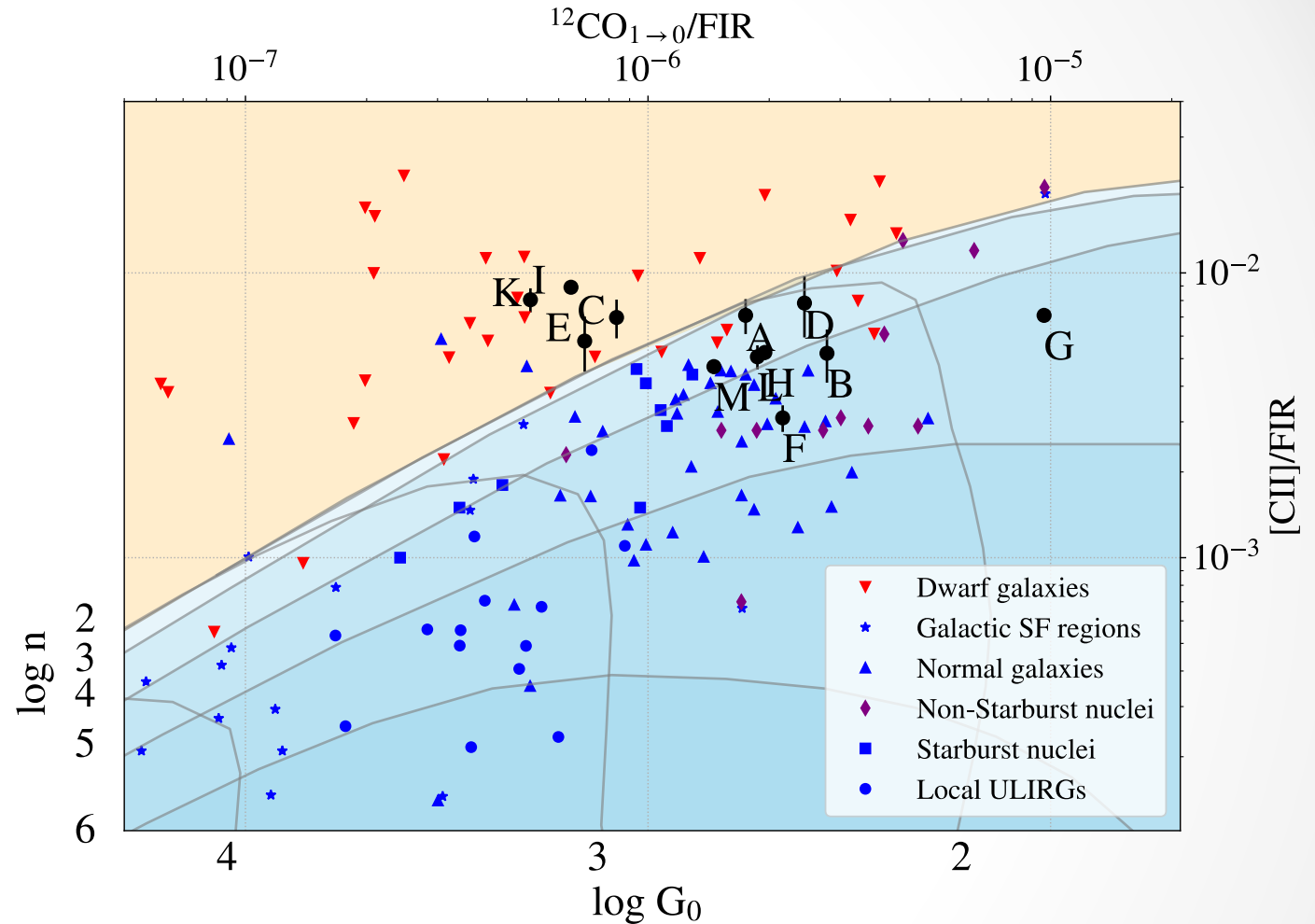


# CO vs [CII]

Normal galaxies populate the blue part of the [CII]/CO diagram. The yellow part contains low metallicity regions and dwarf galaxies.

The grid shows the values of gas density ( $n$ ) and strength of the FUV field ( $G_0$ ) from the PDR models of Kaufman+ 1999.

The local galaxies plotted are from a collection of Madden+ 2020.



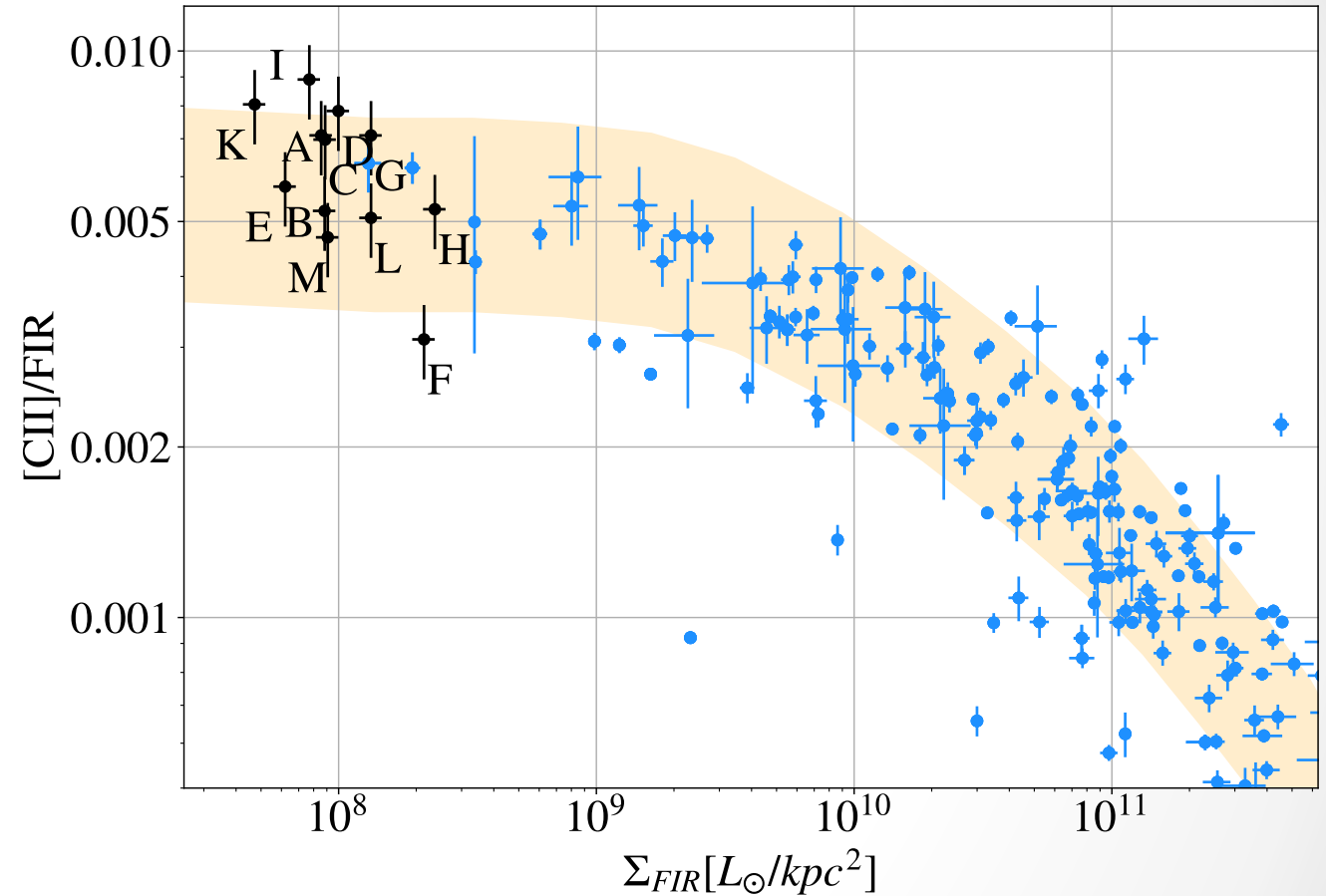
Galaxy compilation from Madden+ 2020

The ratio of [CII]/CO is anomalous in four spots: at the end of the jets, on the north of the nucleus and in a spot outside of the bar.

# [CII] vs FIR

[CII] is a good tracer of SF in normal galaxies. In luminous galaxies, the ratio [CII]/FIR is lower.

The [CII] emission in the hot radio/X-ray spot "I" is not compatible with normal star formation.



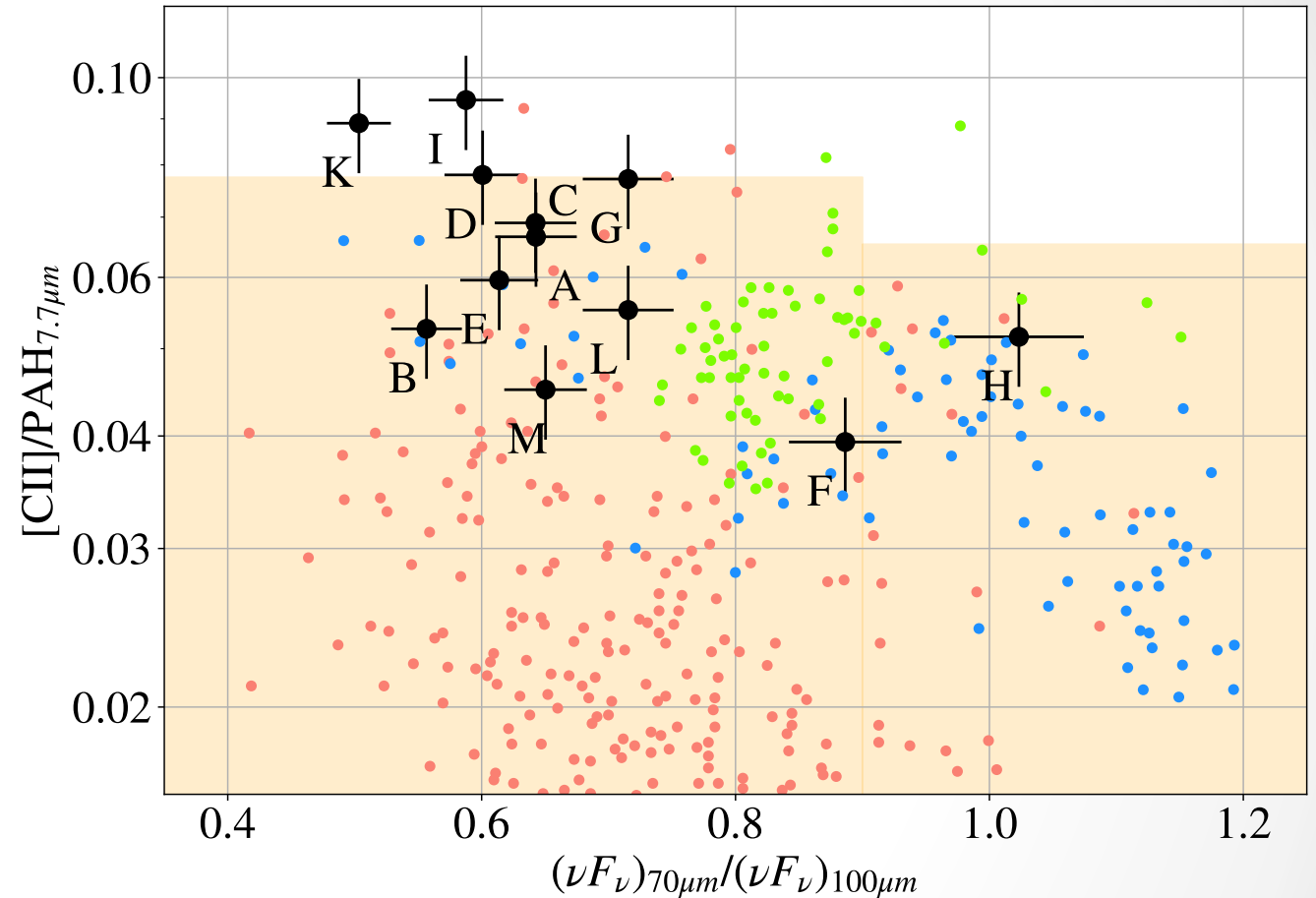
Galaxies (blue dots) and shaded region from Diaz-Santos+ 2017



# [CII] vs PAH emission

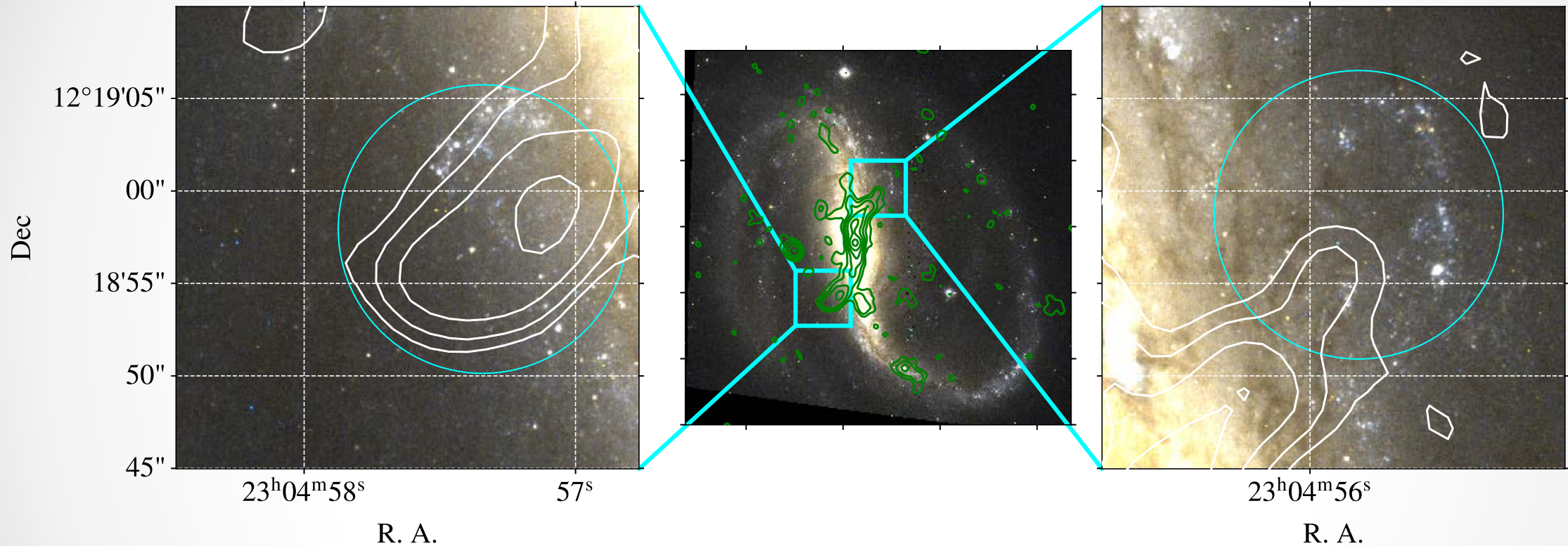
Because PAH are involved in the mechanism of excitation of [CII], if [CII] is due to radiation from stars the [CII]/PAH ratio in galaxy regions is usually found within certain limits.

Two spots in our observations have values exceeding typical values found in other galaxies: the hot radio/X-ray spot "I" and the position out of the bar "K".



Green: NGC 4559 (Croxall + 2012)  
Blue: NGC 1097 (Croxall+ 2012)  
Red: NGC 6946 (Bigiel + 2020)

# Bubbles of star formation



The HST image shows arcs of young blue stars at the end of the jets.  
The northern jet seems to dissipate all the energy in a bubble of stars.  
The southern jet has no star formation at the end, probably because it leaves the disk of the galaxy.  
We speculate that this region emits in [CII] because [CII] is excited by a slow velocity shock similarly to what happened in the galaxy NGC 4258 (Appleton+ 2019).

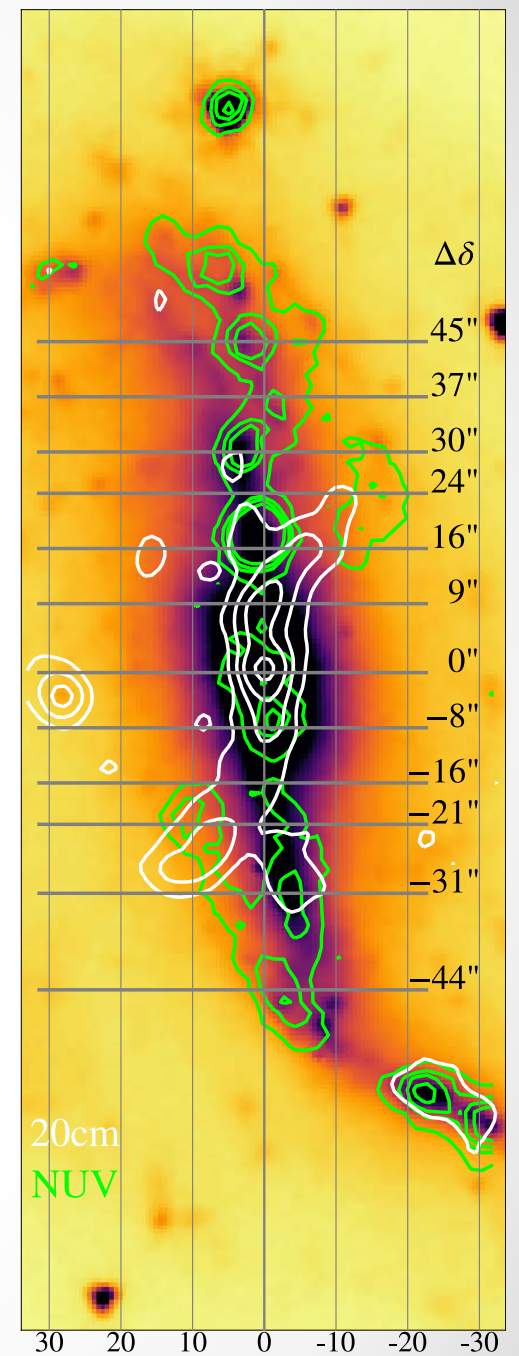
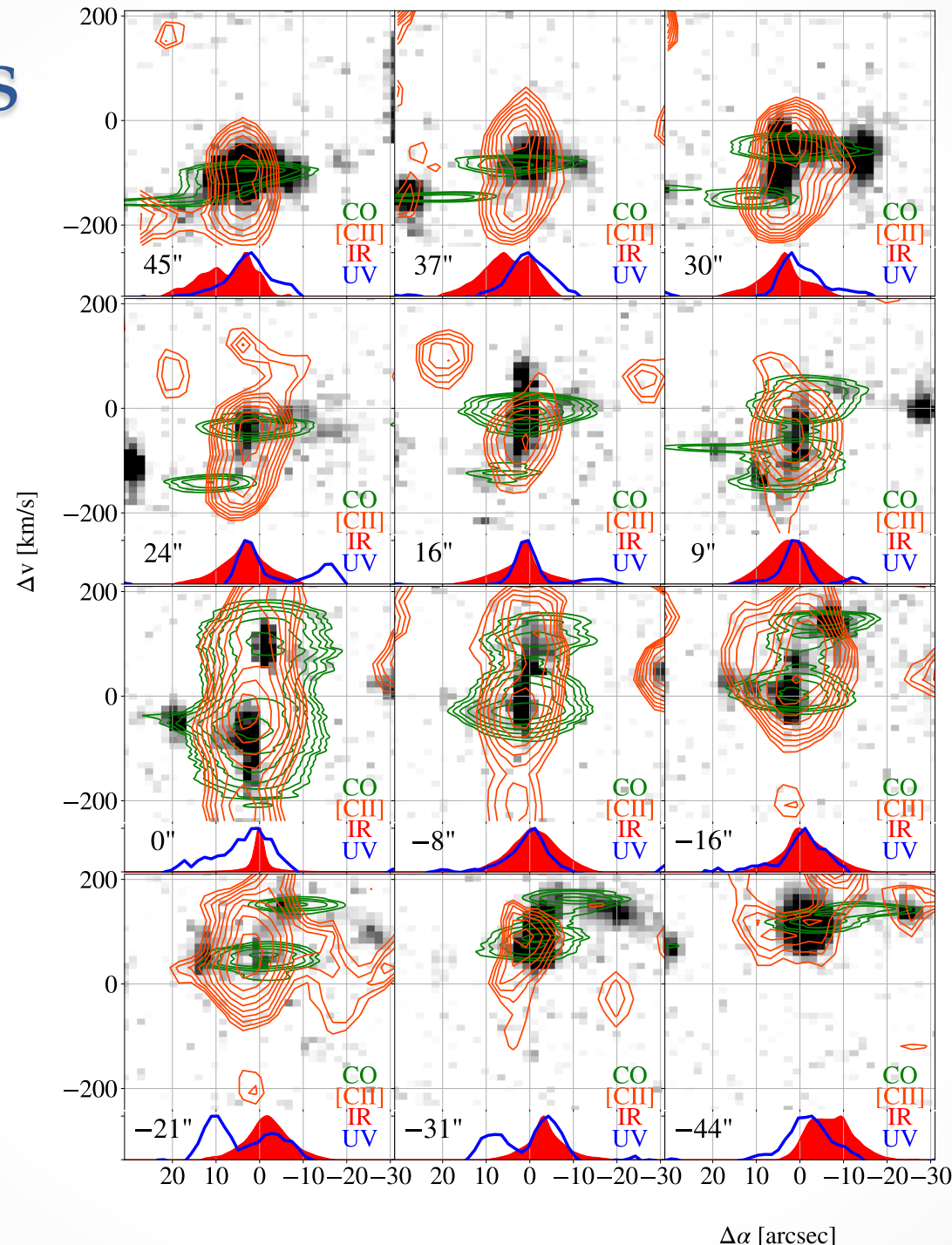
# Gas kinematics

Sections of the [CII], CO, and H $\alpha$  spectral cubes along the bar.

The grey image is the H $\alpha$  cube. CO and [CII] contours are green and orange.

The histogram of IR and UV fluxes along the cuts is at the foot of each diagram.

The emission shows several components.





# Velocity diagrams

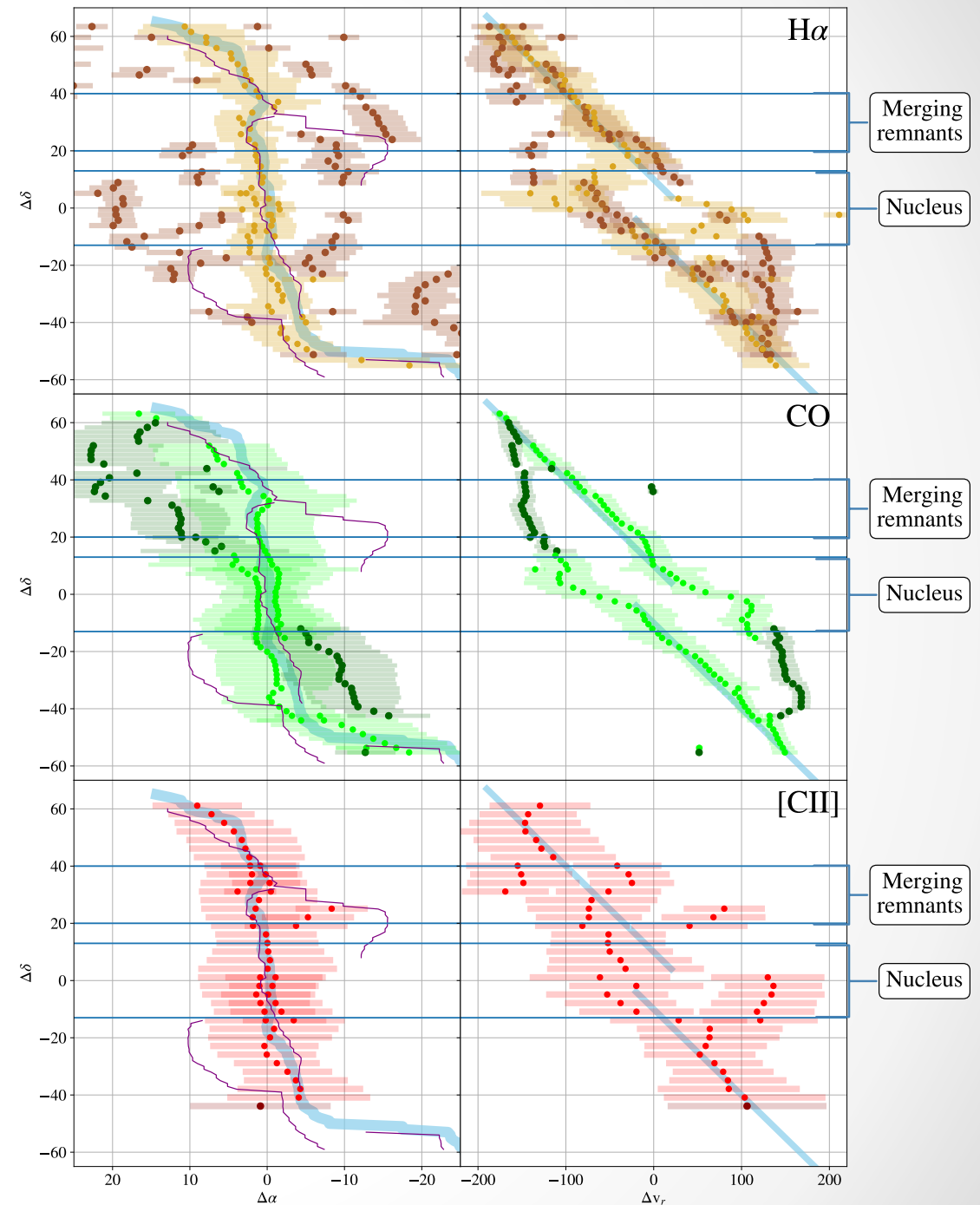
Location and velocity of components of gas emission. Darker colors show components far from the bar more than 5 arcsec.

In the left panels, the location of the bar is traced by the 70 $\mu$ m peak (blue thick line). The peak of UV emission is traced with a thin purple line.

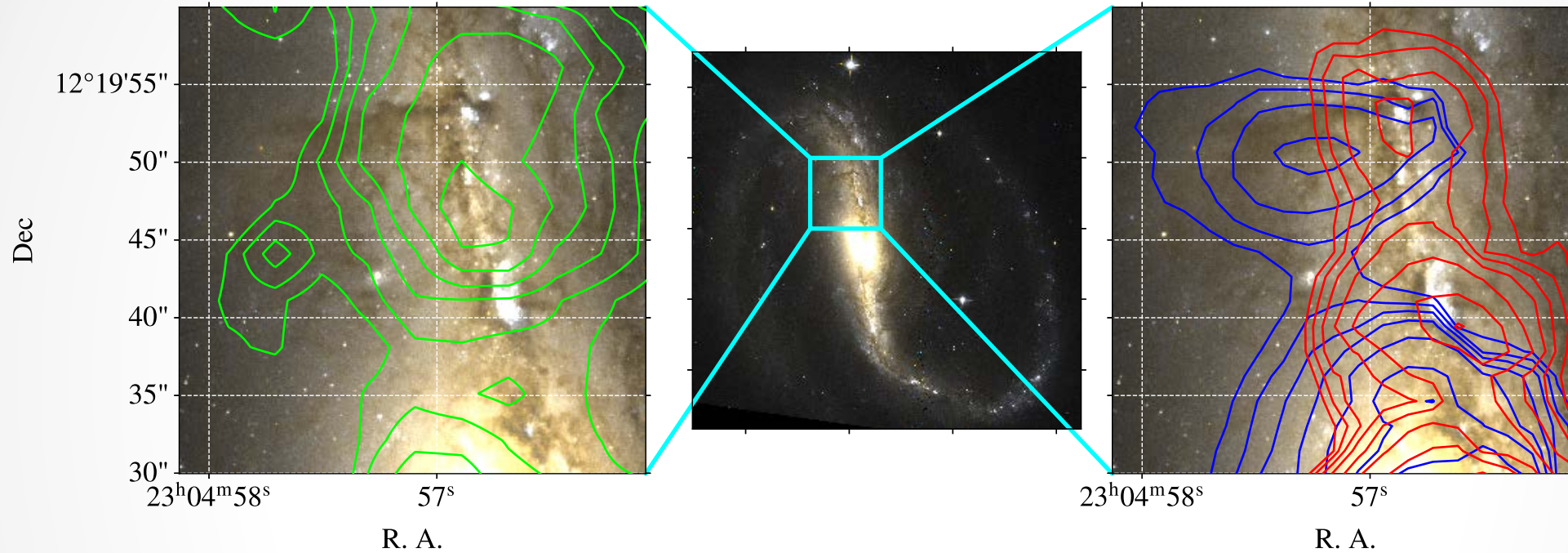
In the right panels, the radial velocities of different components are shown as a function of the declination along the bar. A blue line shows the rigid rotator velocity of the bar.

The CO components just outside the bar trails the bar in the sense of the galaxy rotation. The velocity of these components roughly corresponds to the rotation curve of the galaxy (as shown in the H-alpha emission).

[CII] has a double peak in the merging remnant location.



# Merging remnants



A region north of the nucleus shows remnants of the minor merging, namely the nucleus of the minor galaxy and residuals of an arm.

The [CII] (left) shows strong emission and a double peak in velocity.

The CO emission can be decomposed in two velocity peaks: one along the bar (red) and another trailing the bar (blue). A cloud of molecular gas is found along or limited by the horizontal dust lane.

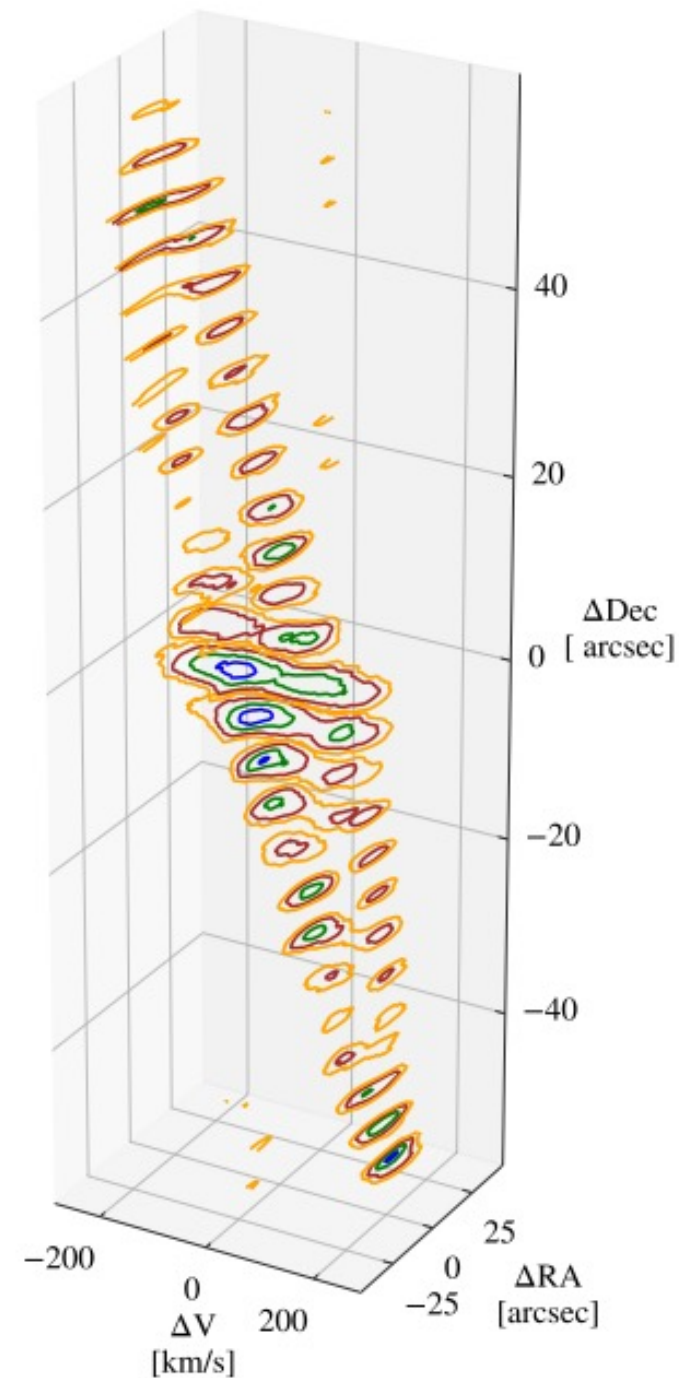
The mass of this cloud is approximately  $10^8 M_{\odot}$ .

# CO velocity peaks

The CO spectral cube shows two distinct peaks.

Thanks to high spectral resolution of the ALMA data, we were able to split the emission in two cubes by fitting Voigt functions to each peak.

The main component is the gas along the bar.  
The other component is gas outside of the bar in a location trailing the bar in the sense of the galaxy rotation.





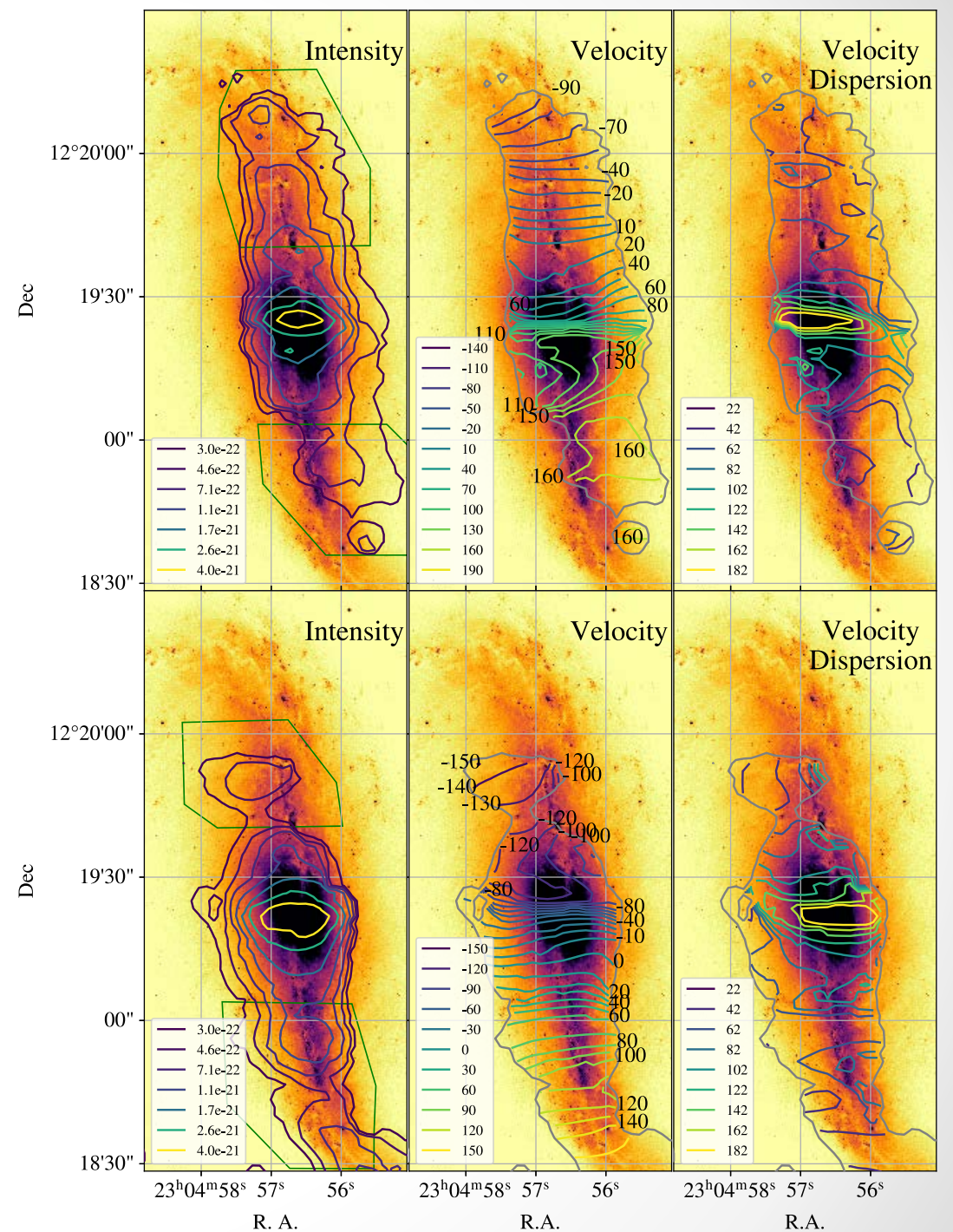
# CO components

When splitting the two components, the gas along the bar has velocity gradients along the bar. The component outside the bar has gradients toward the bar.

The nucleus shows the highest velocity dispersion.

The trailing component amounts to 40% of the gas along the bar (see green polygonal regions). Laine (1998) shows that some of this gas can form during the bar forming process. It could be linked to a minor merging.

A massive cloud ( $\sim 10^8 M_{\odot}$ ) in the north is located along a thick dust lane, a feature related to the minor merging.



# Summary

- We confirm the nuclear origin of the counter-arm emission detected in the radio through the analysis of X-ray Chandra data. The X-ray emission in the southern spot exceeds the emission expected from a pure star-forming region.
- Most of [CII] emission corresponds to CO emission along the bar, showing that it originates from the heating of molecular gas in PDRs due to stellar radiation. There are a few exceptions:
  - At the southern end of the jet a [CII] excess is probably due to cooling of molecular gas shocked by the jet.
  - A region with low CO/[CII] ratio and low metallicity is found outside the bar, probably a patch of CO-dark gas.
- [CII] and CO show resolved kinematical components:
  - [CII] has two components in a region with remnants of the minor merging.
  - CO is detected along the bar and in a region trailing the bar in the sense of the galaxy rotation. The amount of gas in these regions is not negligible: 40% of the gas contained in the bar. A massive cloud ( $\sim 10^8 M_{\odot}$ ) in the north is located along a thick dust lane, a feature related to the minor merging. The origin of the trailing gas could be related to the minor merging.

# On sale


gettyimages

BROWSE PRICING

BOARDS CART SIGN IN

Search the world's best creative photos and images

Creative Images Search by image



gettyimages  
Robert Gendler/Stocktrek Images

153941598

### PURCHASE A LICENSE

All Royalty-Free licenses include global use rights, comprehensive protection, simple pricing with volume discounts available ?

|   |          |
|---|----------|
| <input type="radio"/> Extra small   | \$50.00  |
| <input type="radio"/> Small   | \$175.00 |
| <input type="radio"/> Medium  | \$375.00 |
| <input checked="" type="radio"/> Large<br>3180 x 3274 px (10.60 x 10.91 in)<br>300 dpi   10.4 MP                                      | \$499.00 |
| <input type="radio"/> Market-freeze<br>Protect your creative work - we'll remove this image from our site for as long as you need it. |          |

**\$499.00 USD**

GET THIS IMAGE FOR \$450

ADD TO CART



Dario Fadda  
SOFIA Teletalk - 27 Jan 2021

